

Supplementary Information

Multifunctional core-shell CaSnO₃@N-doped carbon coaxial nanocables with excellent lithium storage performance and efficient microwave absorption

Xiaoqiang Li ^{*,a,b}, Guangguang Guan ^c, Siyi Tong ^a, Xin Chen ^a, Kaiyin Zhang ^d, Jun Xiang ^{*,a}

^a School of Science, Jiangsu University of Science and Technology, Zhenjiang 212100, PR China

^b Institute of Materials Science and Engineering, Beijing University of Technology, Beijing 100124, PR China

^c Shenyang National Laboratory for Materials Science, Institute of Metal Research, Chinese Academy of Sciences, Shenyang 110016, PR China

^d College of mechanical and electrical engineering, Wuyi University, Wuyishan 354300, PR China

*Corresponding author.

E-mail address: Lixq@emails.bjut.edu.cn (X.Q. Li); jxiang@just.edu.cn (J. Xiang).

The model construction and excitation configuration of RCS simulation.

The size dimensions of the perfect electrical conductor (PEC) plate are 180.0 mm × 180.0 mm with a thickness of 0.035 mm. The absorber has the same size dimensions of 180.0 mm × 180.0 mm with PEC plate but a different thickness of 2.5 mm. The far-field position is set to “calculate the field in the direction of the incident plane wave”. The polarization mode employed is linear. The following formula is used to perform the RCS calculation [1, 2]:

$$\sigma \text{ (dB m}^2\text{)} = 10 \log \left[\frac{4\pi S}{\lambda^2} \left| \frac{E_s}{E_i} \right|^2 \right]$$

where S , λ , E_s and E_i are the area of simulation model, the wavelength of EM wave, the scattered electric field intensity and the incident electric field intensity, respectively.

Figures:

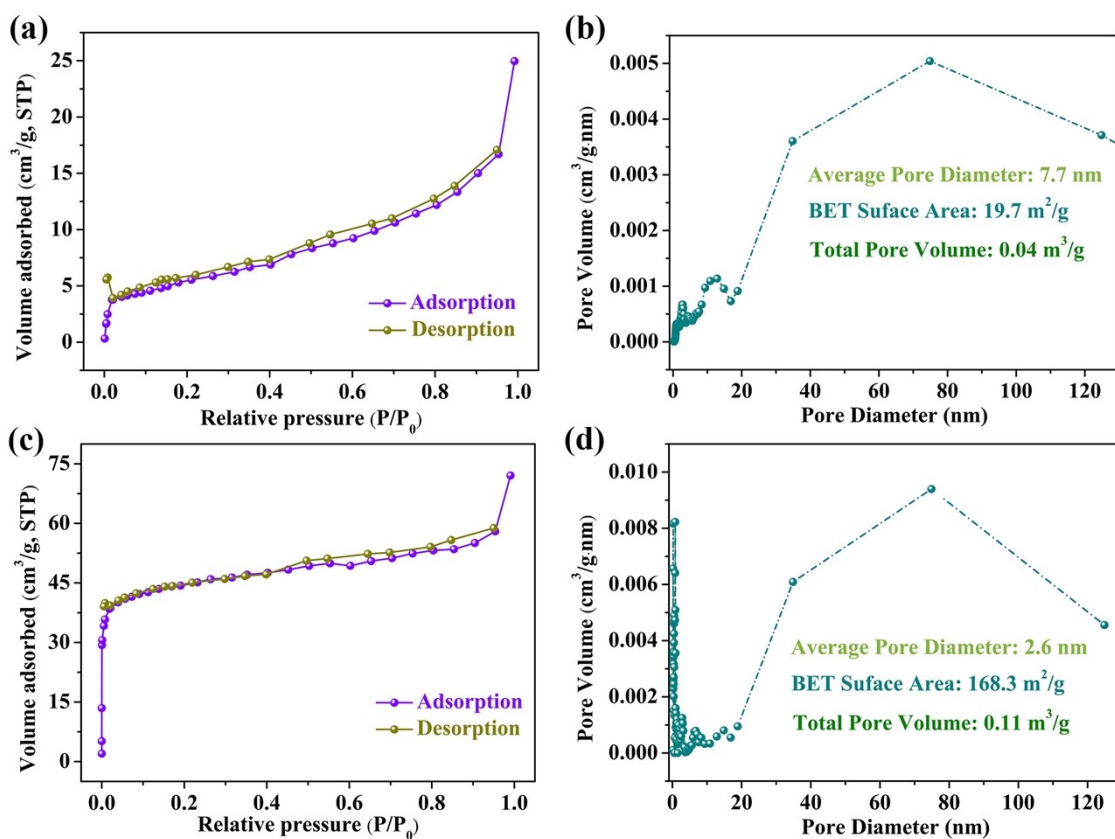


Fig. S1. N₂ adsorption-desorption isotherms and relevant pore size distributions of (a,b) CSONFs and (c,d) CSO@NCNFs-2.

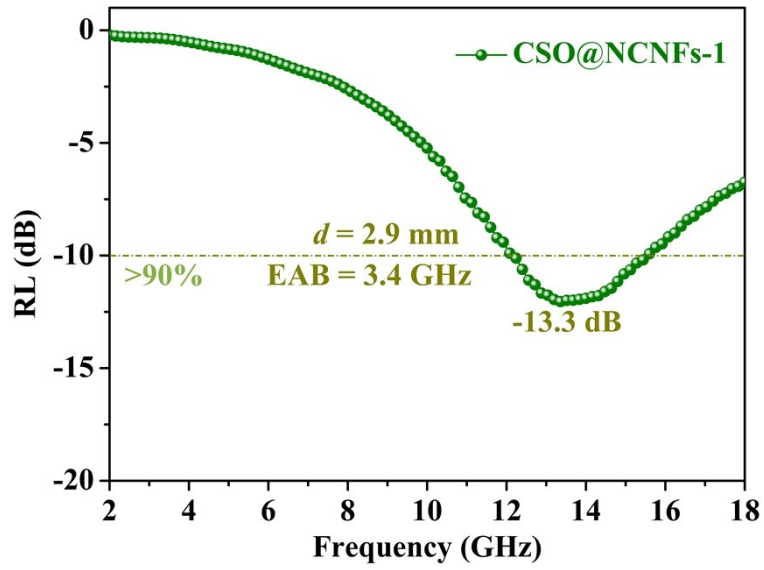


Fig. S2. RL curve and EAB of CSO@NCNFs-1 with an absorber thickness of 2.9 mm.

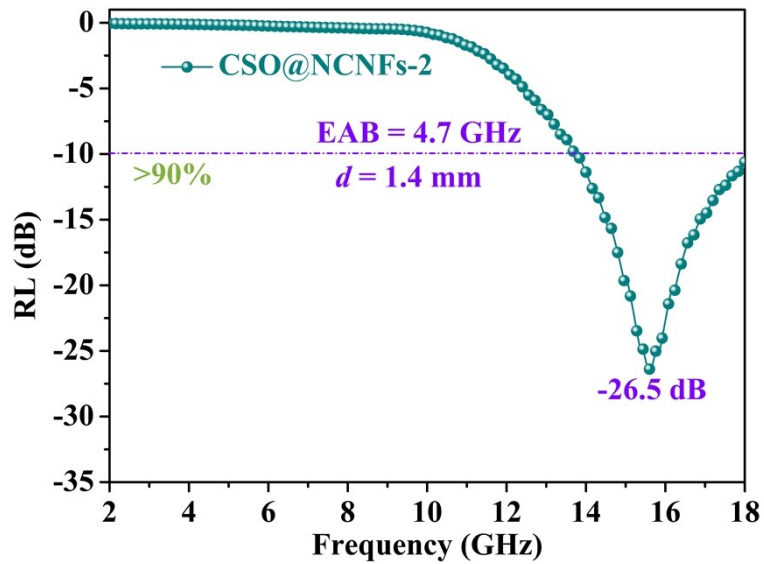


Fig. S3. RL curve and EAB of CSO@NCNFs-2 at an absorber thickness of 1.4 mm.

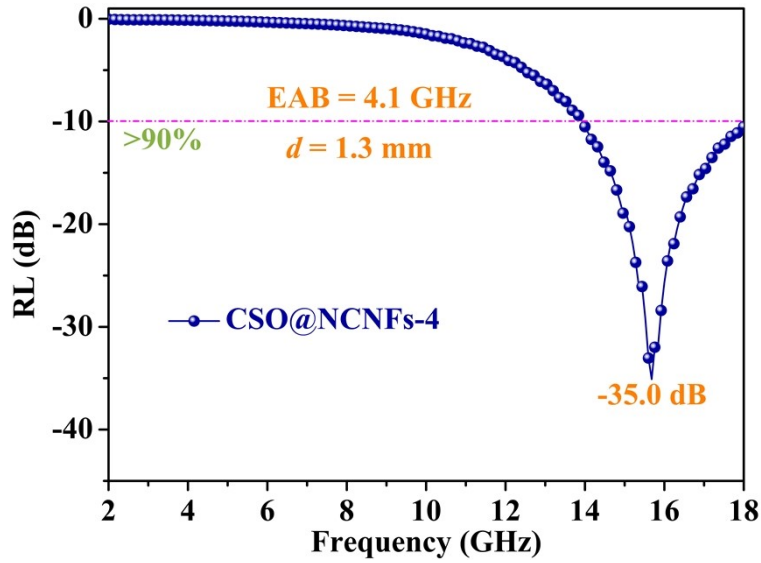


Fig. S4. RL curve and EAB of CSO@NCNFs-4 for an absorber thickness of 1.3 mm.

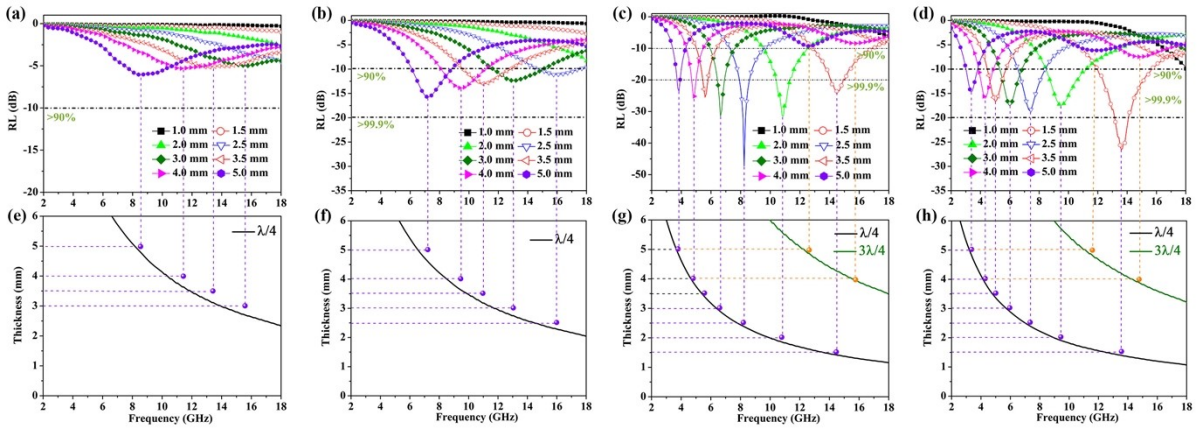


Fig. S5. Frequency dependence of RL values for (a) CSONFs, (b) CSO@NCNFs-1, (c) CSO@NCNFs-2 and (d) CSO@NCNFs-4 samples at different thicknesses. Simulations of matching thickness and peak frequency for (e) CSONFs, (f) CSO@NCNFs-1, (g) CSO@NCNFs-2 and (h) CSO@NCNFs-4 samples under $\lambda/4$ and $3\lambda/4$ models.

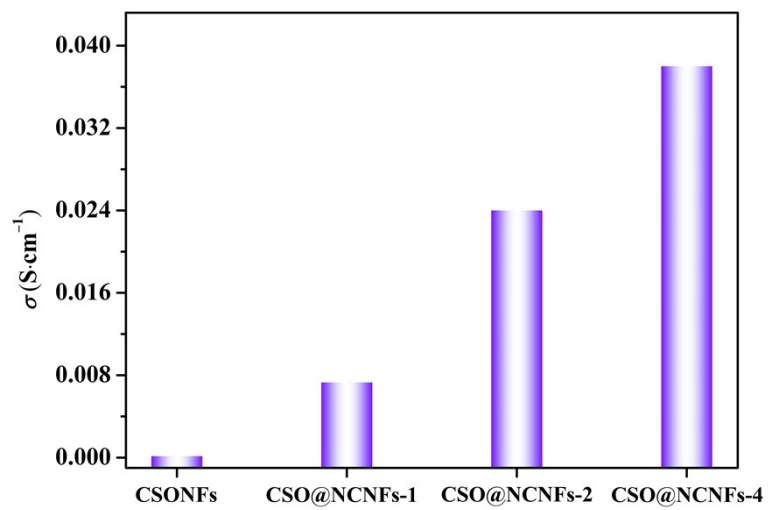


Fig. S6. Electrical conductivity (σ) of CSONFs, CSO@NCNFs-1, CSO@NCNFs-2 and CSO@NCNFs-4.

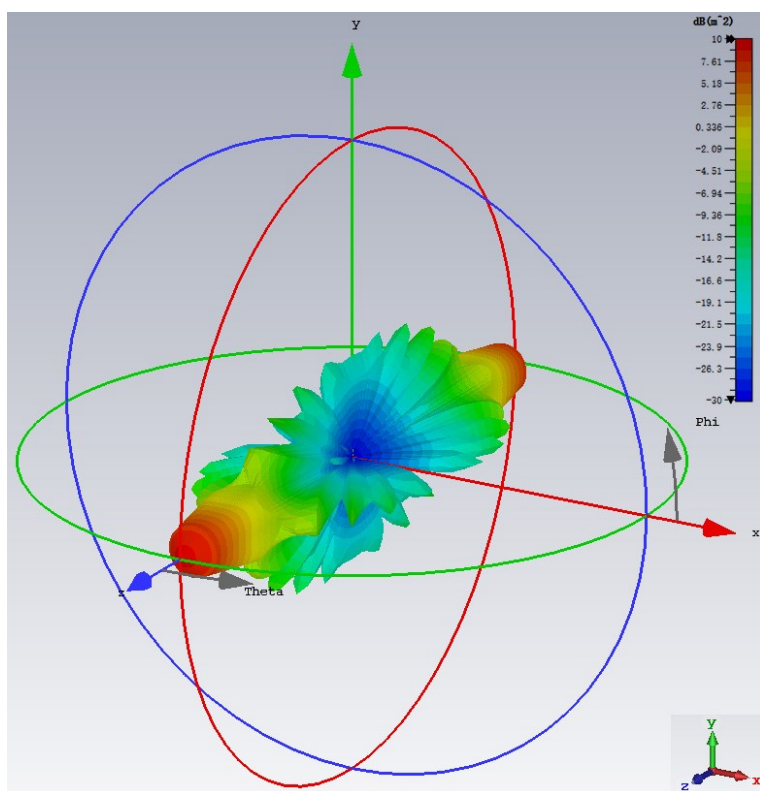


Fig. S7. CST simulation result of PEC.

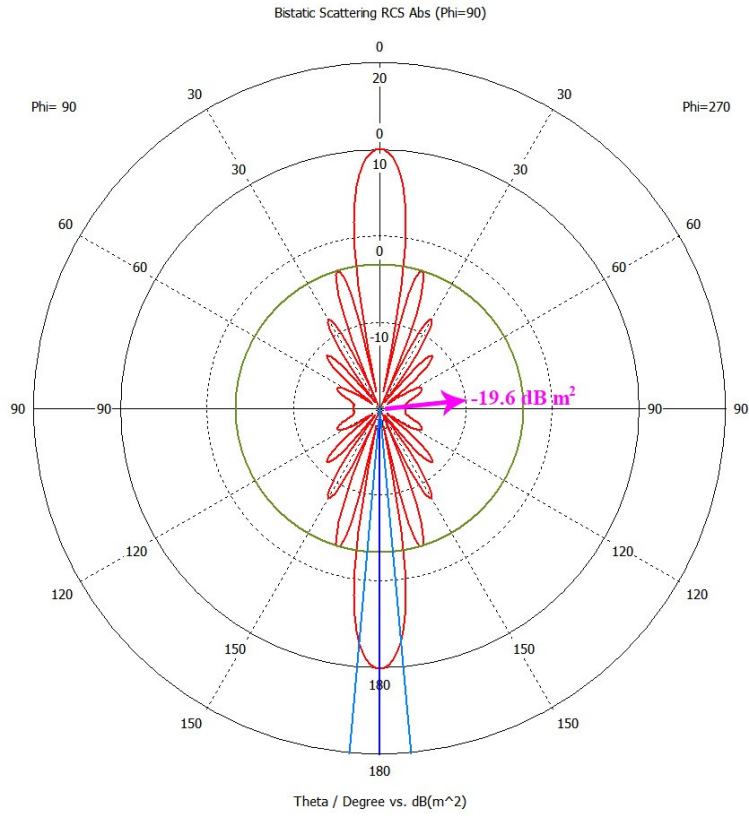


Fig. S8. Polar curve of RCS value for PEC.

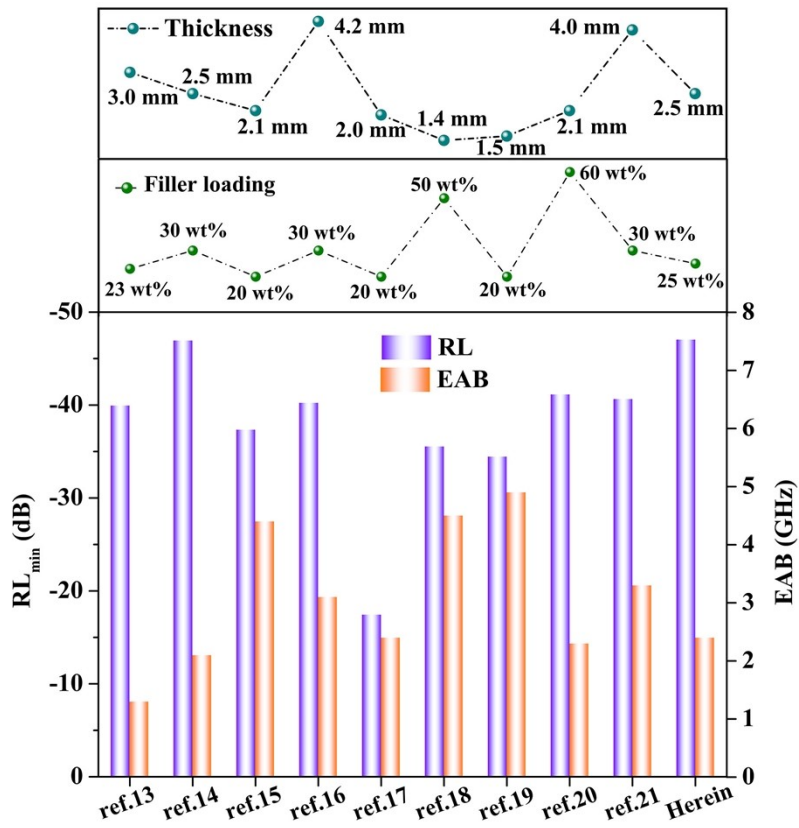


Fig. S9. Comparison of RL_{min}, EAB and filling ratio of some recently reported microwave absorbers.

Tables:

Table S1 Comparison of lithium storage performances of CSO@NCNFs-2 and other CaSnO₃-based and carbon-based electrode materials.

electrode	Current rate	Capacity (mA h g ⁻¹)	Capacity retention	CE	Cycles	Ref.
CSO-nanotubes	60 mA g ⁻¹	648	~56.3%	98.1%	50	[3]
Porous flowerlike CSO	60 mA g ⁻¹	547	~31.3%	99%	50	[4]
C-CTO NTs	60 mA g ⁻¹	~170	~13.1%	/	30	[5]
Nano-CSO	60 mA g ⁻¹	~450	~38.8%	~98%	30	[6]
CSO-NTs-700	60 mA g ⁻¹	565	~48.4%	97.5%	50	[7]
N-doping carbon fiber	1C	~200	~39.2%	/	150	[8]
WO ₃ -26.36%/carbon	100 mA g ⁻¹	540	~36.5%	~99%	150	[9]
CNS-3	100 mA g ⁻¹	~468	~47.8%	~99%	200	[10]
O-MCN-150	100 mA g ⁻¹	197.7	63.2%	63%	100	[11]
Ca ₂ Fe ₂ O ₅ nanofibers-800	50 mA g ⁻¹	530	~50.1%	~98%	100	[12]
CSO@NCNFs-2	100 mA g ⁻¹	645.2	53.7%	99%	100	herein

References

- [1] X.T. Chen, Z.D. Wang, M. Zhou, Y. Zhao, S.L. Tang, G.B. Ji, Multilevel structure carbon aerogels with 99.999 % electromagnetic wave absorptivity at 1.8 mm and efficient thermal stealth, *Chem. Eng. J.* 425 (2023) 139110.
- [2] Y.S. Cao, R.F. Wang, X.Y. Liu, T.R. Zhang, F. Fan, Y. Huang, Multifunctional graphene/carbon fiber aerogels toward compatible electromagnetic wave absorption and shielding in gigahertz and terahertz bands with optimized radar cross section, *Carbon* 199 (2022) 333–346.
- [3] L.L. Li, S.J. Peng, Y.L. Cheah, J. Wang, P.F. Teh, Y. Ko, C.L. Wong, M. Srinivasan, Electrospun eggroll-like CaSnO₃ nanotubes with high lithium storage performance, *Nanoscale* 5 (2013) 134–138.
- [4] S. Zhao, Y. Bai, W.F. Zhang, Electrochemical performance of flowerlike CaSnO₃ as high capacity anode material for lithium-ion batteries, *Electrochim. Acta* 55 (2010) 3891–3896.
- [5] X.Y. Hu, T. Xiao, W. Huang, W. Tao, B.J. Heng, X.Q. Chen, Y.W. Tang, Synthesis, characterization of core–shell carbon-coated CaSnO₃ nanotubes and their performance as anode of lithium ion battery, *Appl. Surf. Sci.* 258 (2012) 6177–6183.
- [6] Y. Sharma, N. Sharma, G.V.S. Rao, B.V.R. Chowdari, Studies on nano-CaO•SnO₂ and nano-CaSnO₃ as

- anodes for Li-ion batteries, *Chem. Mater.* 20 (2008) 6829–6839.
- [7] L.L. Li, S.J. Peng, J. Wang, Y.L. Cheah, P. Teh, Y. Ko, C.L. Wong, M. Srinivasan, Facile approach to prepare porous CaSnO_3 nanotubes via a single spinneret electrospinning technique as anodes for lithium ion batteries, *ACS Appl. Mater. Interfaces*, 4 (2012) 6005–6012.
- [8] Y.N. Kim, Y.K. Lee, C. Tewari, Y. Kim, S. Lee, Y.C. Jung, Simultaneous recycling and nitrogen doping in carbon fiber reinforced plastic using eco-friendly supercritical water treatment for Li-ion batteries anode application, *Carbon* 221 (2024) 118944.
- [9] S.J. Ren, J.G. Huang, A three-dimensional fibrous tungsten-oxide/carbon composite derived from natural cellulose substance as an anodic material for lithium-ion batteries, *Electrochim. Acta* 473 (2024) 143465.
- [10] F. Shi, B.L. Xing, H.H. Zeng, H. Guo, X.X. Qu, G.X. Huang, Y.J. Cao, P. Li, L.H. Feng, C.X. Zhang, Facile synthesis of ultrathin carbon nanosheets through NaCl-KCl templates coupled with ice-induced assembly strategy from carbon quantum dots as lithium-ion batteries anodes, *J. Alloys Compd.* 976 (2024) 173325.
- [11] W. Cha, S. Kim, P. Selvarajan, J.M. Lee, J.M. Davidraj, S. Joseph, K. Ramadass, I.Y. Kim, A. Vinu, Nanoporous carbon oxynitride and its enhanced lithium-ion storage performance, *Nano Energy*, 82 (2024) 105733.
- [12] S.K. Sundriyal, Y. Sharma, Controlled generation and tuning the oxygen defects in nanofibers of $\text{Ca}_2\text{Fe}_2\text{O}_5$ toward high and stable Li-ion battery anode, *Appl. Surf. Sci.* 560 (2021) 150055.
- [13] S.J. Liu, J. Wang, B. Zhang, X.G. Su, X. Chen, Y.H. Chen, H. Yang, Q.L. Wu, S. Yang, Transformation of traditional carbon fibers from microwaves reflection to efficient absorption via carbon fiber microstructure modulation, *Carbon* 219 (2024) 118802.
- [14] X. Li, Z.Z. Zhang, L. Chen, J.M. Zhang, W.S. Chen, R. Feng, X.X. Wang, Multifunctional $\text{MnFe}_2\text{O}_4/\text{TiO}_2/\text{Ti}_3\text{C}_2\text{T}_x$ composites based on in-situ grown TiO_2 for efficient microwave absorption, high hydrophobicity, and heat dissipation properties, *J. Colloid Interface Sci.* 654 (2024) 96–106.
- [15] Y. Cheng, K. Zhou, Y.Z. Ma, H.Q. Zhao, H.B. Yang, Microstructure design of magnetic-dielectric MCHS@Co@CNTs composites with tunable conductive loss for high-performance microwave absorption, *J. Alloys Compd.* 980 (2024) 173641.
- [16] X.F. Yang, M.M. Liu, Y.Q. Lan, L.S. Wu, R. Ji, G.X. Tong, P.J. Gong, Cu^{2+} induced self-assembly of urchin-like $\text{Co}_{1-x}\text{Cu}_x$ into hollow microspheres toward wideband and thin microwave absorbers, *Chem. Eng. J.* 426 (2021) 130779.
- [17] V.K. Chakradhary, M.J. Akhtar, Highly coercive strontium hexaferrite nanodisks for microwave absorption and other industrial applications, *Compos. Part B* 183 (2020) 107667.

- [18] Y. Guo, H.P. Lu, X. Jian, Heterogeneous interface engineering of N-doped carbon onion nanotube chains toward prominent microwave absorption, *Ceram. Int.* 50 (2024) 8030–8041.
- [19] Z.B. Jiao, W.J. Huyan, J.R. Yao, Z.J. Yao, J.T. Zhou, P.J. Liu, Heterogeneous ZnO@CF structures and their excellent microwave absorbing properties with thin thickness and low filling, *J. Mater. Sci. Technol.* 113 (2022) 166–174.
- [20] W.H. Gu, B. Quan, X.H. Liang, W. Liu, G.B. Ji, Y.W. Du, Composition and structure design of Co₃O₄ nanowires network by nickel foam with effective electromagnetic performance in C and X band, *ACS Sustainable Chem. Eng.* 7 (2019) 5543–5552.
- [21] L.H. Wang, S.L. Su, Y.D. Wang, Fe₃O₄–graphite composites as a microwave absorber with bimodal microwave absorption, *ACS Appl. Nano Mater.* 5 (2022) 17565–17575.